An improved compression factor particle swarm optimization-unscented particle filter algorithm for accurate lithium-ion battery state of energy estimation.

HAO, X., WANG, S., FAN, Y., LIANG, Y., WANG, Y. and FERNANDEZ, C.

2023

An improved compression factor particle swarm optimization-unscented particle filter algorithm for accurate lithium-ion battery state of energy estimation

Xueyi Hao[a], Shunli Wang[a*b], Yongcun Fan[a], Yawen Liang[a], Yangtao Wang[a], Carlos Fernandez[c]

[a]*School of Information Engineering, Southwest University of Science and Technology, Mianyang 621010, China;*

[b]*Colledge of Electrical Engineering, Sichuan University, Chengdu, 610065, China;*

[c]*School of Pharmacy and Life Sciences, Robert Gordon University, Aberdeen AB10-7GJ, UK.*

Abstract: Accurate prediction of the remaining range remains a challenge for electric vehicles. The state of energy (SOE) is a state parameter representing the remaining range and remaining charge of a lithium-ion battery, which is related to the prediction of the remaining range of electric vehicles. To obtain the mathematical description and SOE parameters of lithium-ion batteries with high accuracy, a parameter identification method using an improved particle swarm optimization algorithm with compression factor is proposed. For the estimation of energy state, a particle filter (PF) is constructed in this paper, and the unscented particle filtering (UPF) algorithm with particle swarm optimization (PSO) is used to achieve the estimation of energy state, which can solve the problems of particle degradation and insufficient particle diversity of particle filtering. The experimental results show that the SOE estimation error is within 0.97% at 25 degrees for all three operating conditions and within 1.29% at 5 degrees for all three operating conditions. Therefore, the proposed algorithm has high accuracy and strong robustness at different temperatures and different working conditions, and the estimation results prove the validity of energy state estimation.

Keywords: state of energy, unscented particle filtering, particle swarm optimization, parameter

identification

1 Introduction

In recent years, as the global economy continues to grow and problems such as resource scarcity and environmental pollution become more serious, the development of clean and renewable energy has become a global issue, and green and healthy new energy sources have gradually entered people's vision and become the focus of scholars' research [1-3]. Among them, lithium-ion batteries are widely used in new energy vehicles, aerospace, rail transportation, and other high-end emerging industries due to their high voltage, high specific energy, long cycle life, good safety performance, self-discharge, and so on. In the second quarter of 2022, lithium-ion batteries, electronic components, integrated circuits, and other industry segments will have a value-added growth rate of more than 20%. With the increasing market demand for lithium-ion batteries and expanding application areas, the safety, and reliability of lithium batteries have become an important research topic [4, 5].

The lithium-ion battery is a system with highly nonlinear operating characteristics. The acquisition and modeling of time-varying parameters inside the lithium-ion battery is an important factor affecting the accurate characterization of the lithium-ion battery and the accurate estimation of the energy state [6]. To effectively establish the state-space expressions of lithium-ion batteries, equivalent models with high adaptability must be established [7-9]. The equivalent circuit model can represent the ohmic internal resistance and open-circuit voltage characteristics of the battery [10, 11], which can reflect the relevant parameters inside the lithium-ion battery from a macroscopic perspective and can be used to study the influence of charge/discharge open-circuit voltage discrepancy, which is simple to calculate compared with the above two models [12], so the equivalent circuit model is chosen for this paper. Thevenin model, second-order RC equivalent model [13-16], PNGV model, and fractional-order model [17, 18] have been widely used in extensive research by scholars at home and abroad [9, 12, 19]. In this paper, after considering the cost and computing power of BMS, the second-order RC equivalent model is chosen as the research object.

The state of energy is both an important parameter to measure the performance of power

batteries and a key basis to develop control strategies [20-22]. The SOC, as we know it, refers to the remaining charge margin in the battery, which can protect the battery from overcharging and discharge and prolong its service life. SOE reflects the degradation of the battery [23-26], which is mainly expressed as the decline of the available capacity and the increase of the ohmic internal resistance [27-30]. Accurate estimation of SOE is beneficial to enhance the management and control of power battery systems and improve the utilization efficiency of power batteries [31-35]. The literature [36] proposed a Particle Filter-Extended Kalman Filter (PF-EKF) algorithm to estimate SOE to improve the accuracy and robustness of SOE estimation; the literature [37] combined the equivalent circuit model with the Unscented Particle Filter algorithm to deal with model nonlinearity, The literature [38] used two interrelated particle filters to simultaneously implement the equivalent model parameter identification and SOE estimation, which partially attenuated the impact of the time-varying equivalent parameters on the SOE estimation accuracy; the literature [39] proposed a dual filtering algorithm based on the extended Kalman filter and particle filter to establish an online energy state estimator based on the model. The results show that the model can better simulate the battery dynamics and the convergence of the algorithm is good.

Currently, particle filtering techniques have been successfully applied to many fields such as target tracking, computer vision, and fault diagnosis [40]. However, a common problem in basic particle filtering algorithms is the degeneracy phenomenon, which is because the variance of particle weights increases with time iterations [41-43]. The degeneracy phenomenon is inevitable and after several iterations, the weights of all but a few particles are negligible. The degeneracy means that if the drop in generations continues, then a large number of computational resources are consumed in dealing with those insignificant particles. To solve the problem, the following aspects can be improved: the first method is to increase the number of particles, increasing the number of particles is also called increasing the sampling points, the number of particles, naturally, can fully reflect the diversity of particles, can slow down the degeneration, but the number of computing increases. The second method is to improve the proposed density function, the premise assumptions of the basic particle filtering: importance resampling can be sampled from a reasonable posterior proposed density distribution to get a set of sample points set, and this set of sample points set can cover the real state well. If these

assumptions are not satisfied, the effect of the particle filtering algorithm has to be reduced; therefore, if an optimal proposed density distribution function can be found to guide the resampling to do the correct sampling distribution, then the validity of the sample set can be guaranteed, and the final quality of the filtering can be ensured. The third method is the optimization of the resampling method. the essence of resampling is to increase the diversity of particles. SIR particle filtering does this more successfully than SIS particle filtering. The introduction of the resampling mechanism avoids the possibility of losing the diversity of particles.

Therefore, in this paper, a particle swarm optimization algorithm [44] optimized unscented particle filtering algorithm is proposed for energy state estimation, using an unscented Kalman filter (UKF) as the proposed density function of particle filtering to solve the problem of particle degradation of particle filtering, followed by the introduction of particle swarm optimization algorithm to improve the resampling link of particle filtering and increase the particle diversity to solve the problem of lack of particle diversity of particle filtering.

The first chapter introduces the current background and status of the lithium battery energy state; the second chapter introduces the theoretical knowledge based on this paper, including the establishment of the equivalent model, the introduction of the particle swarm optimization algorithm and its improvement algorithm, and the description of the particle swarm optimization traceless particle filtering algorithm; the third chapter describes the comparison and analysis of the results based on the proposed algorithm and other existing algorithms under different complex working conditions; the fourth chapter is the conclusion of this paper, which demonstrates the superiority of the proposed algorithm and its limitations.

2 Mathematical

2.1 Equivalent Circuit Model

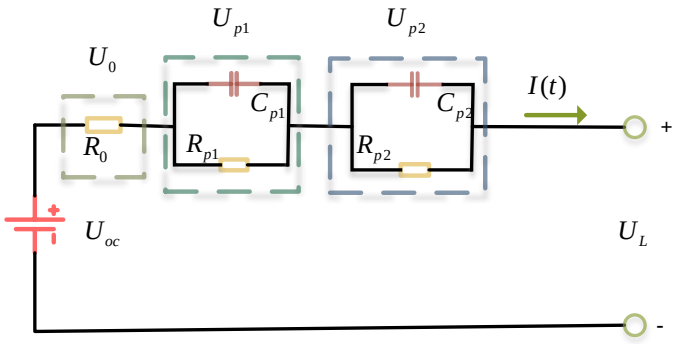

Figure 1 Second-order RC equivalent model

As shown in Figure 1, the second-order RC equivalent model is obtained by adding an RC parallel loop to the Thevenin model. In the figure, the RC loop composed of R_{p1} and C_{p1} represents the stage of rapid voltage change during the chemical reaction inside the battery; the RC loop is composed of R_{p2} and C_{p2} represents the stage of slow voltage change during the chemical reaction inside the battery. The simple model is easy to calculate, but cannot accurately describe the operating characteristics of the battery. The complex model can better characterize the charging and discharging characteristics of the battery, but the calculation volume will be greatly increased, which reduces the adaptability and promotion of the model. The effects of different orders of equivalent circuit models on the SOE estimation effect are compared, among which, the second-order RC equivalent model is more accurate and the computational effort, although a bit larger than the Thevenin and PNGV models, is within the acceptable range. Taking this into account, this paper decides to use the second-order RC equivalent model for SOE estimation. According to Kirchhoff's current law as well as the voltage law, equation (1) can be obtained.

$$\begin{cases} U_L = U_{oc}(SOC) - i(t)R_0 - U_{p1} - U_{p2} \\ \dfrac{dU_{p1}}{dt} = -\dfrac{U_{p1}}{R_{p1}C_{p1}} + \dfrac{i}{C_{p1}} \\ \dfrac{dU_{p2}}{dt} = -\dfrac{U_{p2}}{R_{p2}C_{p2}} + \dfrac{i}{C_{p2}} \end{cases} \tag{1}$$

In equation (1), U_{oc} represents the terminal voltage, R_0 represents the internal resistance of the second-order RC equivalent model, while R_{p1}, R_{p2} represent the polarization resistance, C_{p1}, C_{p2} represent the polarization capacitance, and U_{p1}, U_{p2} refer to the voltages of the two RC loops, respectively. Combined with the definition of SOE, equation (1) is discretized and $[SOC\ U_{p1}\ U_{p2}]$ is selected as the state variable to obtain the state space expression for the second-order RC equivalent model, as shown in equation (2).

$$\begin{cases} \begin{bmatrix} SOE_{k+1} \\ U_{p1,k+1} \\ U_{p2,k+1} \end{bmatrix} = \begin{bmatrix} 1 & 0 & 0 \\ 0 & 1 - \dfrac{T}{\tau_1} & 0 \\ 0 & 0 & 1 - \dfrac{T}{\tau_2} \end{bmatrix} \\ U_{L,k+1} = U_{oc} - U_{p1} - U_{p2} - IR_0 \end{cases} \tag{2}$$

In equation (2), the parameters to be identified in the model are $R_0, R_{p1}, C_{p1}, R_{p2}, C_{p2}$, and the specific parameter identification method and the parameter identification process will be described in detail below.

2.2 Particle Swarm Optimization Algorithm

Particle Swarm Optimization is a stochastic search algorithm based on group collaboration developed by simulating the foraging behavior of a flock of birds. It is usually considered a kind of swarm intelligence (SI). The particle swarm optimization algorithm was invented by Dr. Eberhart and Dr. Kennedy. The PSO algorithm simulates the foraging behavior of a flock of birds. Suppose a flock of birds is searching for food randomly and there is only one piece of

food in the area. All the birds do not know where the food is. But they know how far their current position is from the food. So what is the optimal strategy to find the food? The simplest and most effective one is to search the area around the bird closest to the food.

PSO takes inspiration from this model and uses it to solve optimization problems in which the solution to each optimization problem is a bird in the search space. We call them "particles". All particles have a fitness value determined by the function being optimized, and each particle has a velocity that determines the direction and distance they fly. The particles then follow the current optimal particle and search the solution space.

Parameter identification methods include offline identification methods, online identification methods, and intelligent identification, by comparing the advantages and disadvantages of several identification methods, we choose to use the PSO algorithm of intelligent methods as the basic algorithm of parameter identification. Figure 2 shows the flow chart of the PSO algorithm.

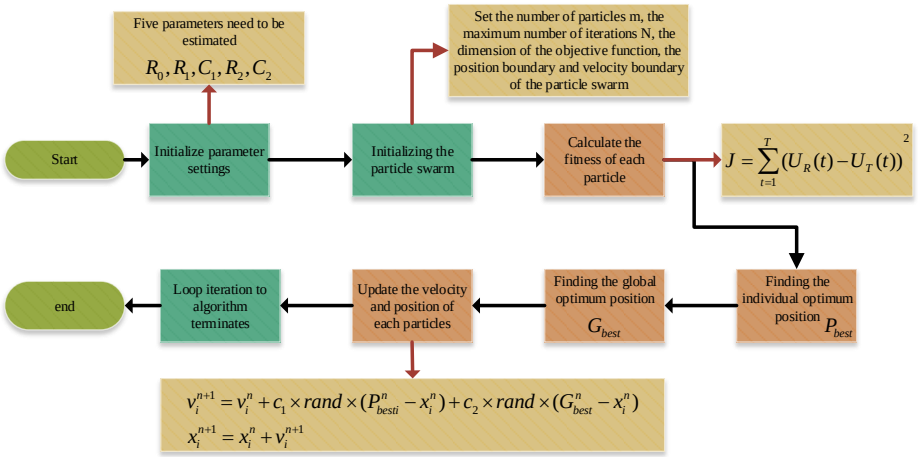

Figure 2 The flow of the PSO algorithm

The PSO is initialized as a population of random particles (random solutions) and then iterates to find the optimal solution. In each iteration, the particles update themselves by

tracking two "extremes". The first one is the optimal solution found by the particle itself, which is called the individual extreme value $pBest$, and the other extreme value is the optimal solution found by the whole population, which is the global extreme value $gBest$. Alternatively, instead of using the entire population, one can just use the neighbors of some of the optimal particles, and then the extreme value among all neighbors is the local extreme value. When these two optimal values are found, the particle updates its velocity and new position according to equation (3).

$$\begin{aligned} v_i^{n+1} &= \omega v_i^n + c_1 \times rand \times (P_{besti}^n - x_i^n) + c_2 \times rand \times (G_{best}^n - x_i^n) \\ x_i^{n+1} &= x_i^n + v_i^{n+1} \end{aligned} \tag{3}$$

At present, the PSO algorithm has been widely used in function optimization, neural network training, pattern assignment, fuzzy control, and other fields. However, PSO algorithms also have defects such as poor local search ability, easy falling into local extremes, and low search accuracy. Therefore, the improvement of the PSO algorithm becomes a key challenge.

2.3 Compression Factor Particle Swarm Optimization Algorithm

To remove the limitation of the particle velocity boundaries and accelerate the convergence of the PSO algorithm, Clerc et al. introduced the compression factor into the basic PSO algorithm, and the introduction of the compression factor can change the velocity of the particles. The compression factor λ is calculated as shown in equation (4).

$$\lambda = \frac{2}{|2 - \varphi - \sqrt{(\varphi^2 - 4\varphi)}|} \tag{4}$$

Where $\varphi = c_1 + c_2$, the individual learning factor c_1 and the social learning factor c_2 determine the influence of the particles' empirical information and the empirical information of

other particles on the trajectory of the particles, which reflects the information exchange among the particle population. A larger value of c_1 will cause the particles to search too much in their local range, while a larger value of c_2, in turn, will drive the particles to converge to the local optimum prematurely. Figure 3 details the flowchart of the particle swarm optimization algorithm after adding the compression factor.

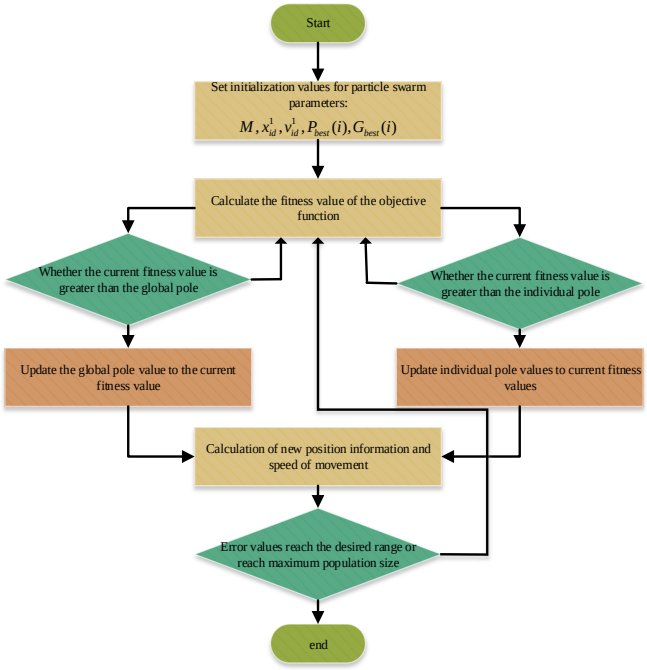

Figure 3 The flow of the CFPSO algorithm

The CFPSO algorithm with the addition of the compression factor has the velocity and position calculated as shown in equation (5).

$$v_i^{n+1} = \lambda \times (\omega v_i^n + c_1 \times rand \times (P_{besti}^n - x_i^n) + c_2 \times rand \times (G_{best}^n - x_i^n)) \quad (5)$$

$$x_i^{n+1} = x_i^n + v_i^{n+1}$$

2.4 Improved Compression Factor Particle Swarm Optimization Algorithm

After adding the compression factor, the CFPSO algorithm achieves a balance between global search and local search to some extent. However, another important parameter in the

CFPSO algorithm, the value of ω, is a fixed value, that represents the inertia weight of the particle itself. But the solution details of the problem change as the number of iterations increases, and the fixed value has many defects in the overall solution process. Thus, to dynamically adapt to the problem-solving process, this paper introduces adaptive inertia weights. Therefore, this paper presents a new ICFPSO algorithm, Figure 4 introduces the flow of this algorithm.

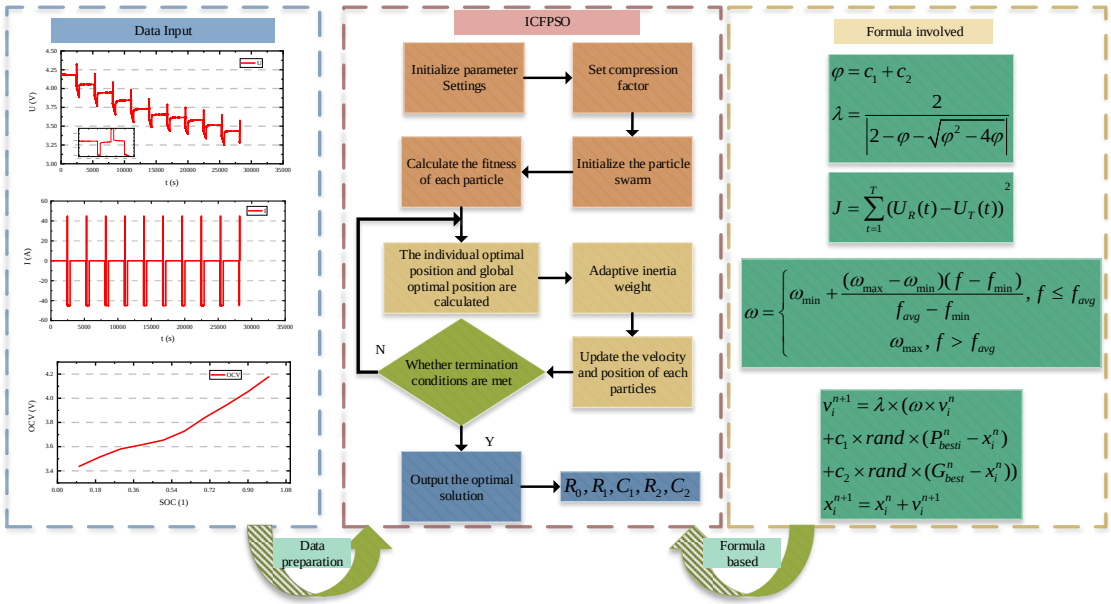

Figure 4 The flow of the ICFPSO algorithm

A larger inertia weight facilitates the global search and a smaller inertia weight facilitates the local search. The improved velocity and position update process is consistent with equation (5), however, the value of ω in equation (5) is no longer a fixed value, but dynamically changing, and its change process is shown in equation (6).

$$\omega = \begin{cases} \omega_{min} + \dfrac{(\omega_{max} - \omega_{min})(f - f_{min})}{f_{avg} - f_{min}}, f \le f_{avg} \\ \omega_{max}, f > f_{avg} \end{cases} \quad (6)$$

In this paper, we take $\omega_{max} = 0.9, \omega_{min} = 0.4$, when the first iteration is larger ω, the algorithm has a strong global search capability, with the increase of the number of iterations, ω

is smaller when the algorithm conducts a more accurate local search.

2.5 Unscented particle filter based on improved particle swarm optimization

SOE is an important part of the research on lithium-ion batteries. SOE reflects the deterioration degree of batteries and is a state parameter representing the remaining battery life and remaining power of lithium-ion batteries. Its definition is shown in equation (7).

$$SOE(k+1) = SOE(k) + \frac{\int_k^{k+1} \eta P(k) dk}{E_T} \tag{7}$$

In equation (7), $SOE\ (k+1)$ represents the energy status value of the next moment, $SOE\ (k)$ represents the energy status value of the current moment, $P\ (k)$ is the power of the lithium-ion battery, E_T is the rated energy of the battery.

The unscented Kalman filter algorithm is used as the proposed density function for particle filtering to solve the problem of particle degradation in particle filtering, followed by the introduction of an improved particle swarm optimization algorithm to optimize the resampling link of the particle filtering algorithm to solve the problem of lack of particle diversity in the particle filtering algorithm. As a result, the improved particle swarm optimization unscented particle filtering algorithm proposed in this paper is formed, and the flow chart of this algorithm is shown in Figure 5.

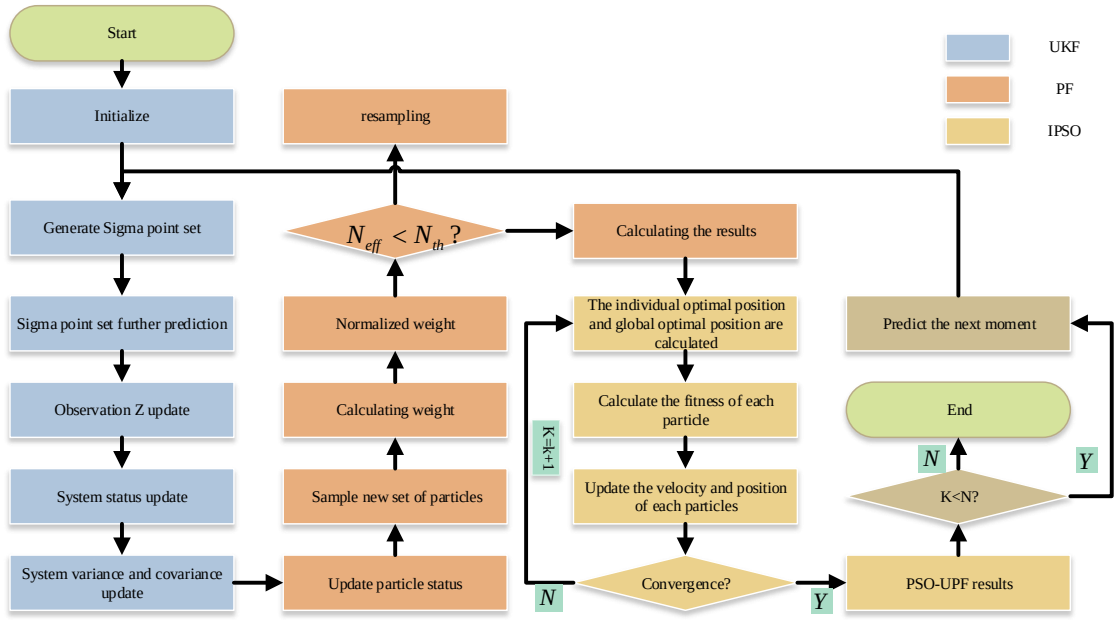

Figure 5 The flow of the IPSO-UPF algorithm

The basic flowchart of the proposed algorithm is presented as shown in Figure 5, which is described as follows.

(1) Initialization

N particles $\{x_0^i, i = 1,2,\cdots,N\}$ are collected from the prior distribution p(x_0), so that the initial weight of each sample is $w_0^i = \frac{1}{N}, i = 1,2,\cdots,N$.

(2) Significance sampling

Update the particle $\{x_{k-1}^i, p_{k-1}^i\}$ states with the UKF algorithm, update and thus obtain $\{\tilde{x}_k^i, p_k^i\}$; find the mean $\bar{x}_k^i$ and variance $\delta_{x_k}^i$ of the particle set $\{\hat{x}_k^i\}_{i=1}^N$; sample particle x_k^i from the importance density function $q\left(\frac{x_k}{x_{k-1}^i}, Z_k\right) = N(\hat{x}_k^i, \bar{x}_k^i, \delta_{x_k}^i)$.

(3) Weight update

The weights are calculated: $\tilde{w}_{k-1}^i \frac{p(z_k/x_k^i)p(x_k^i/x_{k-1}^i)}{q(\frac{x_k^i}{x_{k-1}^i}, Z_k)}$, and the weights are normalized: $w_k^i = \frac{\tilde{w}_k^i}{\sum_i \tilde{w}_k^i}$.

(4) Resampling

Resampling condition is determined: $N_{eff} = \frac{1}{\sum_{i=1}^{M}(w_k^i)^2} < N_{th}$, and N_{th} is the threshold value of particle number.

(5) Improving the particle swarm optimization process

Set the objective function as $fitness = \exp\left(-\frac{(voltage-Z)^2}{2R}\right)/\sqrt{2\pi R}$, take the sample set generated by the trackless particle filter as the initial position of the particle swarm, calculate the velocity and position of the particle by equation (3) above, and iteratively update it continuously, when the maximum number of iterations is reached, the search will be stopped.

(6) Output final state value

$$SOE_k = \sum_{i=1}^{M} w_k^i SOE_k^i \tag{8}$$

3 Experiment

3.1 Experimental platform

To ensure the orderly conduct of the experiment, the construction of the experimental platform is of paramount importance. The experimental equipment used in this paper includes a power battery large rate charge/discharge tester (BTS 750-200-100-4), a three-layer independent temperature-controlled high and low-temperature test chamber (BTT-331C), etc. The schematic diagram of the experimental platform is shown in Figure 6.

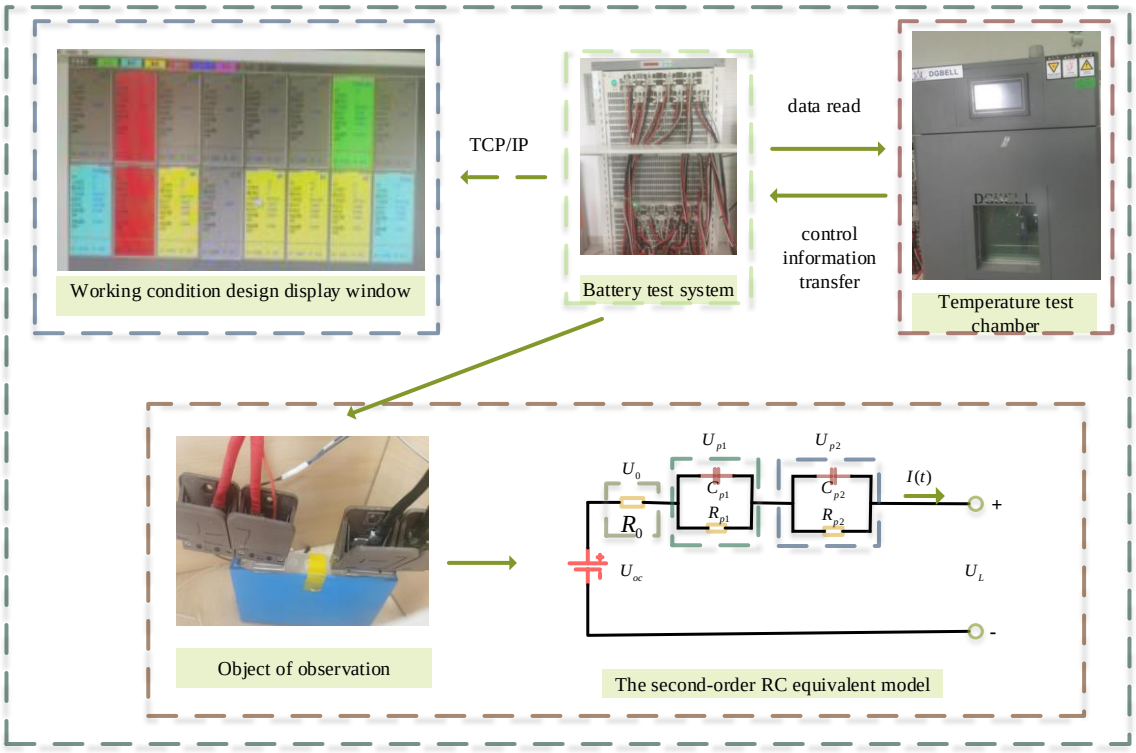

Figure 6 Schematic diagram of the experimental platform

The power battery large multiplier charge/discharge tester is mainly applied to power battery working condition simulation, pulse charge/discharge, cycle life (Cycle Life), multiplier charge/discharge test, etc. The three-layer independent temperature-controlled high and low-temperature test chamber can accurately simulate the complex natural-like environment of low temperature, high temperature, high temperature and high humidity, low temperature, and low humidity, etc. This paper takes the ternary lithium battery as the research object, whose rated capacity is 45Ah.

3.2 Parameter Identification Result

Based on the analysis of the PSO algorithm and its improvement algorithm above, we finally choose the ICFPSO algorithm for the parameter identification of the model. In this paper, to verify the identification effect of the algorithm, Hybrid Pulse Power Characteristic (HPPC)

experiment was carried out with laboratory equipment, and the experimental circuit voltage data were finally obtained. The end voltages calculated from the equivalent circuit model of the battery and the end voltages measured in the laboratory are compared to evaluate whether the model parameters identified by the ICFPSO algorithm can fully characterize the battery. Figure 7 shows the comparison of the simulated and experimental voltages for several algorithms.

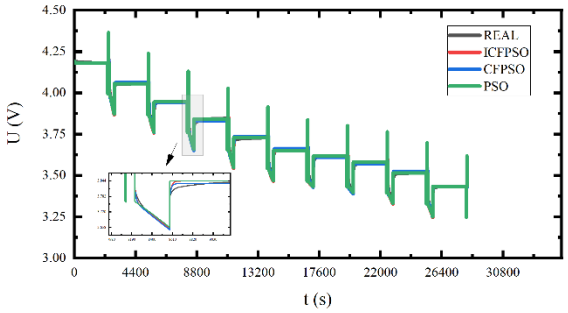

(a-1) Simulated voltage and experimental voltage curves

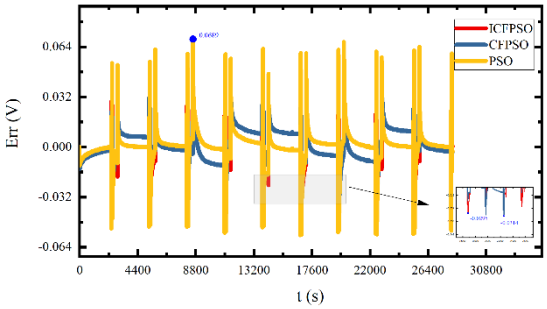

(a-2) Error curve of simulated voltage and experimental voltage

(a) Parameter identification results at 25 degrees

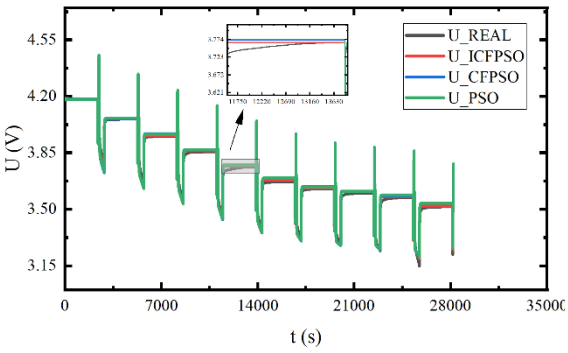

(b-1) Simulated voltage and experimental voltage curves

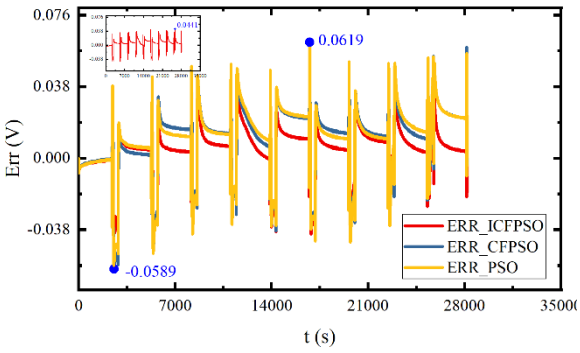

(b-2) Error curve of simulated voltage and experimental voltage

(b) Parameter identification results at 5 degrees

Figure 7 Simulation voltage and experimental voltage curve and error curve

In Figure 7, we can obtain the simulated voltage curves of several parameter identification algorithms, and comparing the simulated voltage with the experimental voltage, we can obtain

the curves shown above, and we can observe that the simulated voltage obtained by the ICFPSO algorithm is closer to the experimental value, and the curve fluctuations are less undulating. To analyze the effect of temperature on parameter identification, HPPC experiments at 25 degrees and 5 degrees are conducted, and by conducting experiments on the centralized parameter identification algorithm at different temperatures, we can obtain the results shown in Figure 7. The results show that the change of temperature will make the estimation of parameter discrimination poor, but the change of temperature does not affect the comparison of the advantages and disadvantages of various parameter discrimination algorithms, and the proposed algorithm still has superiority when the temperature is changed compared with other algorithms. Next, we can specifically analyze the performance indicators of several algorithms to compare the advantages and disadvantages of several algorithms in more detail. Table 1 lists the performance indexes of several algorithms.

Table 1 Performance index of several parameter identification algorithms

Temperature	Algorithm	ME	MAE	RMSE
25℃	ICFPSO	0.0295	0.0042	0.0068
	CFPSO	0.0314	0.0074	0.0089
	PSO	0.0689	0.0047	0.0091
5℃	ICFPSO	0.0441	0.0104	0.0136
	CFPSO	-0.0589	0.0167	0.0196
	PSO	0.0619	0.0171	0.0199

As shown in Table 1, we can calculate the maximum error (ME), the maximum average error (MAE), and the root mean square error (RMSE) of several algorithms. the MAE is the average difference between the predicted and experimental test values. the RMSE indicates the sample standard deviation of the difference between the predicted and observed values, and the

root mean square error, to indicate the dispersion of the sample, is as small as possible. Through the comparison, it can be seen that the ICFPSO algorithm has the best discrimination effect and the smallest error. Calculating the performance metrics of various parameter identification algorithms at 25 degrees and 5 degrees respectively, we can very much find that the decrease in temperature from 25 degrees to 5 degrees deteriorates the performance of several algorithms. However, regardless of the temperature, the proposed algorithm still has a high superiority compared to other algorithms.

To achieve an estimation of SOE, modeling is very important. This paper presents a particle swarm optimization algorithm with compression factor and adaptive inertia weights for parameter identification of the second-order RC model. The results of parameter identification and voltage simulation using this model are given in this paper. ICFPSO algorithm shows that the model and parameter identification algorithm can accurately characterize the battery, and the maximum simulation error of the voltage is 39.4 mV, which is smaller than that of the single particle swarm optimization algorithm.

3.3 The results of HPPC working condition

The HPPC condition contains several cyclic experimental steps such as shelving and intermittent charging and discharging, which have strong dynamicity and can better simulate the working condition of the battery. The initial value of SOE estimation is set to 1, and the experimental data of HPPC condition are used to verify the proposed algorithm and several commonly used algorithms the comparison of experimental results and estimation errors are shown in Figure 8(a) and Figure 8(b), respectively.

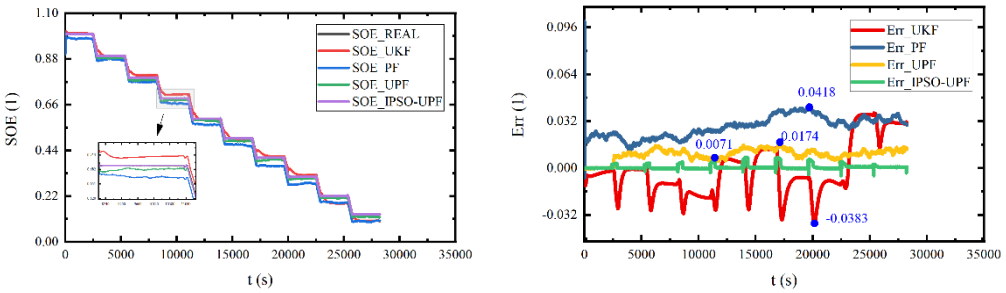

(a-1) SOE estimation curves (a-2) SOE estimation error curves

(a) SOE estimation results and errors under HPPC conditions at 25 degrees

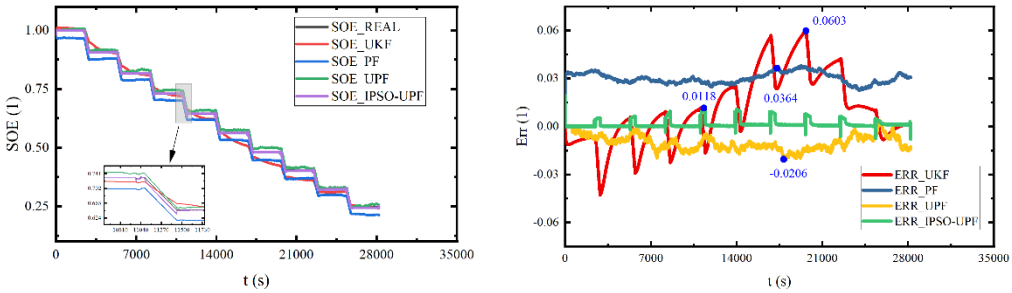

(b-1) SOE estimation curves (b-2) SOE estimation error curves

(b) SOE estimation results and errors under HPPC conditions at 5 degrees

Figure 8 SOE estimation curve and its error curve under HPPC condition

From Figure 8, we can see that the estimation curve of the proposed algorithm is the best fit with the real estimation curve obtained from the experimental test, and there is a certain difference between the estimation curve of other algorithms and that measured by the experiment. By observing the error curves of several algorithms, it can be seen that the error curve of the UKF algorithm fluctuates greatly. The PF algorithm has a slightly smaller fluctuation range, which indicates that it has good stability, but its error is large. Compared with the previous two algorithms, UPF is superior in stability and maximum error value. Based on the UPF algorithm, the proposed algorithm further improves stability and reduces the maximum error value. The temperature has a certain influence on the SOE of lithium-ion batteries, and it can be seen from Figure 8 that the same algorithm has different effects on the estimation of SOE at different temperatures. However, the estimated effect of the proposed algorithm is the best

for both 5 degrees and 25 degrees. Therefore, the proposed algorithm has superiority at multiple temperatures compared with other algorithms.

Table 2 Performance indexes of several algorithms under HPPC conditions

Temperature	Algorithm	MAX	MAE	RMSE
25℃	IPSO-UPF	0.0071	0.0008	0.0016
	UPF	0.0174	0.0094	0.0101
	PF	0.0418	0.0282	0.0182
	UKF	-0.0383	0.0147	0.0290
5℃	IPSO-UPF	0.0118	0.0014	0.0026
	UPF	-0.0206	0.0101	0.0111
	PF	0.0364	0.0302	0.0303
	UKF	0.0603	0.0184	0.0242

Table 2 lists the maximum error values, MAE values and RMSE values of several algorithms. Therefore, compared with Table 2, it can be seen that the parameters obtained after parameter identification using the ICFPSO algorithm are substituted into the IPSO-UPF algorithm for SOE estimation with the best effect. From the perspective of three performance indexes, the values of the three performance indexes of the proposed algorithm are all the minimum, which verifies the stability of the proposed algorithm on the other hand, and further proves the superiority of the proposed algorithm. By comparing the performance metrics of various algorithms at 25 degrees versus 5 degrees under HPPC conditions, we can find that the temperature can affect the SOE estimation results. However, the change in temperature does not change the superior comparison of the algorithms, and the proposed algorithm still has good stability as well as superiority.

3.4 The results of BBDST working condition

The BBDST working condition comes from the actual data collection of the Beijing bus dynamic test, which contains the data under various operations such as starting, coasting, accelerating, rapid acceleration, etc. It is realistic and dynamic, and the actual application working condition of high-power lithium batteries is complex and changeable, so it is more convincing to use BBDST experimental data to verify the feasibility of the algorithm. The effect of SOE estimation under BBDST working conditions is shown in Figure 9.

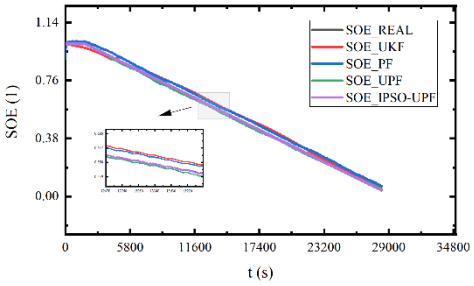

(a-1) SOE estimation curves

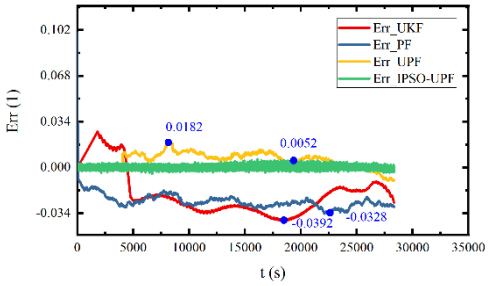

(a-2) SOE estimation error curves

(a) SOE estimation results and errors under BBDST condition at 25 degrees

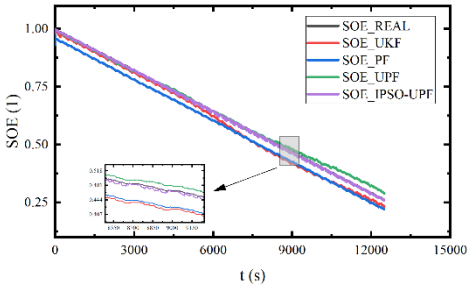

(b-1) SOE estimation curves

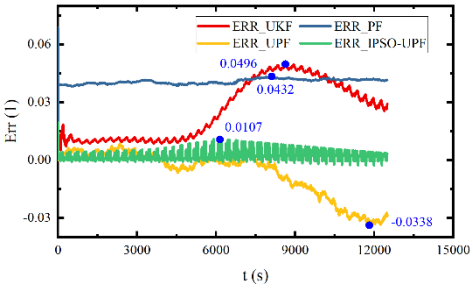

(b-2) SOE estimation error curves

(b) SOE estimation results and errors under BBDST condition at 5 degrees

Figure 9 Estimation results and errors of SOE under BBDST condition

Figure 9 shows the SOE estimation curves and error curves of several algorithms, among which, Figure 9(a) shows the SOE estimation results and corresponding errors at 25 degrees, and Figure 9(b) shows the estimation curve at 5 degrees. As can be seen from Figure 9, several error curves have a high overlap degree in the early stage. After obtaining parameters from the

ICFPSO algorithm and combining the IPSO-UPF algorithm, the error curve of SOE estimation is superior to other algorithms in fluctuation degree. In the later stage, the fluctuation of other algorithms is larger, resulting in a large deviation and obvious error accumulation phenomenon. However, the proposed algorithm has good stability with small fluctuation and the overall stability is within 0.6%. Through the comparison of the four figures, it can be seen that the SOE estimation results obtained by the proposed algorithm are superior to other algorithms no matter in the BBDST working condition of 25 degrees or 5 degrees. In the BBDST working condition, the maximum error value, MAE and RMSE were used to compare the estimated results of several algorithms, as shown in Table 3.

Table 3 Performance index of the algorithm in BBDST condition

Temperature	Algorithm	MAX	MAE	RMSE
25℃	IPSO-UPF	0.0052	0.0009	0.0013
	UPF	0.0182	0.0065	0.0078
	PF	0.0328	0.0253	0.0257
	UKF	0.0392	0.0242	0.0256
5℃	IPSO-UPF	0.0107	0.0027	0.0034
	UPF	-0.0338	0.0092	0.0137
	PF	0.0432	0.0407	0.0408
	UKF	0.0496	0.0257	0.0297

Table 3 describes the performance indexes of several algorithms. According to Table 3, after parameter identification by the ICFPSO algorithm, SOE estimation by the proposed algorithm is better than the UPF algorithm, PF algorithm and UKF algorithm. And, by the change of the performance index of several algorithms after temperature change, we can further determine the superiority of the proposed algorithm. In summary, the proposed algorithm is an

optimal choice.

3.5 The results of DST working condition

In practical applications, the real-time current of lithium-ion batteries is complex and variable. This imposes strict requirements on the dynamic performance of the battery and makes it difficult to estimate the SOE of lithium-ion batteries under complex operating conditions. To further verify the estimation of lithium-ion battery SOE by the estimation model under more complex application conditions, the model is simulated and validated with the experimental data of customized DST conditions.

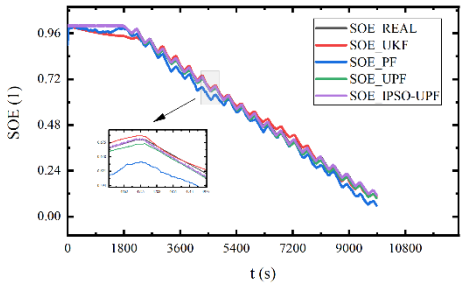

(a-1) SOE estimation curves

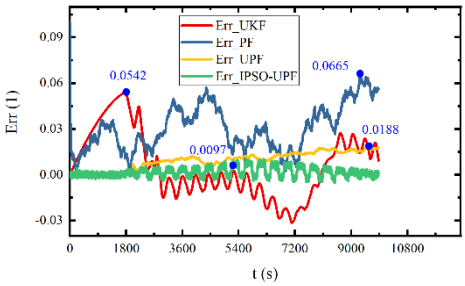

(a-2) SOE estimation error curves

(a) SOE estimation results and errors under DST conditions at 25 degrees

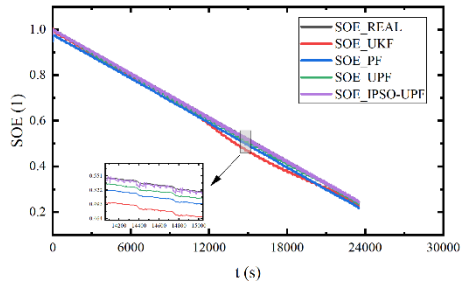

(b-1) SOE estimation curves

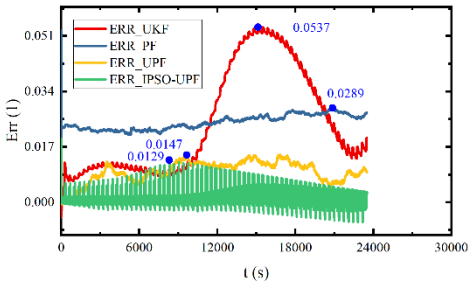

(b-2) SOE estimation error curves

(b) SOE estimation results and errors under DST conditions at 5 degrees

Figure 10 Estimation results and errors of SOE under DST conditions

The estimation curves and corresponding error curves of several algorithms are respectively described in Figure 10. From the curve changes in the figure, we can see that the SOE curve estimated by the combination of the parameter values obtained after parameter

identification of the ICFPSO algorithm and the proposed algorithm has the least fluctuation, better convergence can better track the real value, and the error can be controlled within 1%. The parameter results obtained by the ICFPSO algorithm combined with other algorithms are estimated to be as high as 6.65%, and the error tends to increase significantly. By comparing Figure 10(a) with Figure 10(b), it can be found that the proposed algorithm has the best estimation and the best stability with high accuracy and strong robustness compared with other algorithms in this paper, both at 25 degrees and at 5 degrees. Therefore, we can see that the temperature has some influence on the SOE estimation effect, but the proposed algorithm still has superiority at multiple temperatures. Table 4 lists the performance indicators of several algorithms.

Table 4 Performance index of the algorithm in DST condition

Temperature	Algorithm	MAX	MAE	RMSE
25℃	IPSO-UPF	0.0097	0.0026	0.0034
	UPF	0.0188	0.0094	0.0109
	PF	0.0665	0.0306	0.0399
	UKF	0.0542	0.0175	0.0222
5℃	IPSO-UPF	0.0129	0.0019	0.0025
	UPF	0.0147	0.0095	0.0099
	PF	0.0289	0.0245	0.0246
	UKF	0.0537	0.0241	0.0291

Table 4 lists the performance indicators of several algorithms. As can be seen from the values calculated in Table 4, the values of several performance indicators of SOE estimation using the ICFPSO algorithm for parameter identification and combined with the proposed algorithm are the smallest, which indicates that this estimation algorithm has the best effect,

and the difference between the estimated value and the real value is small, and the following effect is the best. By comparing the performance indexes of several algorithms under two temperatures, it can be further demonstrated that the proposed algorithm outperforms other algorithms and is a good choice for SOE estimation of lithium-ion batteries.

4 Conclusion

To achieve an accurate estimation of SOE, modeling and identification are very important. Based on the second-order RC equivalent model, a new improved compression factor particle swarm optimization algorithm is proposed for parameter identification. The parameter identification results and voltage simulation results of the algorithm are applied in this paper. The simulation results of the ICFPSO algorithm show that the model and parameter identification algorithm can accurately characterize the battery. The maximum error value of the simulation voltage is 29.5 mV, which is smaller than that of the CFPSO algorithm and PSO algorithm. For SOE estimation, an improved particle swarm optimization algorithm-unscented particle filter algorithm is used to estimate the energy state of lithium-ion batteries. Compared with PF, UKF and UPF algorithms, the algorithm used in this paper can estimate SOE better. The IPSO-UPF algorithm can better solve the problem of particle degradation and lack of particle diversity of the PF algorithm. Experimental results show that this algorithm can achieve accurate estimation of SOE well. Next, we will continue to study the joint SOC and SOE estimation algorithm of IPSO-UPF with reduced computational effort, so that the algorithm has higher computational accuracy and operation speed.

Acknowledgments

The work was supported by the National Natural Science Foundation of China (No. 62173281).

Reference

[1]. Li, R., et al., *State of Charge Prediction Algorithm of Lithium-Ion Battery Based on PSO-SVR Cross Validation.* Ieee Access, 2020. **8**: p. 10234-10242.

[2]. Ren, X., et al., *A method for state-of-charge estimation of lithium-ion batteries based on PSO-LSTM.* Energy, 2021. **234**.

[3]. Bian, X., et al., *A Two-Step Parameter Optimization Method for Low-Order Model-Based State-of-Charge Estimation.* Ieee Transactions on Transportation Electrification, 2021. **7**(2): p. 399-409.

[4]. Chen, Y., et al., *Remaining available energy prediction for lithium-ion batteries considering electrothermal effect and energy conversion efficiency.* Journal of Energy Storage, 2021. **40**.

[5]. Shrivastava, P., et al., *Combined State of Charge and State of Energy Estimation of Lithium-Ion Battery Using Dual Forgetting Factor-Based Adaptive Extended Kalman Filter for Electric Vehicle Applications.* Ieee Transactions on Vehicular Technology, 2021. **70**(2): p. 1200-1215.

[6]. Chen, L., et al., *Electrochemical Model Parameter Identification of Lithium-Ion Battery with Temperature and Current Dependence.* International Journal of Electrochemical Science, 2019. **14**(5): p. 4124-4143.

[7]. Wang, Y., et al., *A comprehensive review of battery modeling and state estimation approaches for advanced battery management systems.* Renewable & Sustainable Energy Reviews, 2020. **131**.

[8]. Li, W., et al., *Data-driven systematic parameter identification of an electrochemical model for lithium-ion batteries with artificial intelligence.* Energy Storage Materials, 2022. **44**: p. 557-570.

[9]. Xu, L., et al., *Enabling high-fidelity electrochemical P2D modeling of lithium-ion*

batteries via fast and non-destructive parameter identification. Energy Storage Materials, 2022. **45**: p. 952-968.

[10]. Yanhui, Z., et al., *A Generalized Extended State Observer for Supercapacitor State of Energy Estimation With Online Identified Model.* IEEE Access, 2018. **6**.

[11]. Xie, W., et al., *Unscented Particle Filter Based State of Energy Estimation for LiFePO4 Batteries Using an Online Updated Model.* International Journal of Automotive Technology, 2022. **23**(2).

[12]. Yu, P., et al., *An adaptive fractional-order extended Kalman filtering for state of charge estimation of high-capacity lithium-ion battery.* International Journal of Energy Research, 2022. **46**(4): p. 4869-4878.

[13]. Wang, Z., et al., *A novel method of parameter identification and state of charge estimation for lithium-ion battery energy storage system.* Journal of Energy Storage, 2022. **49**.

[14]. Xie, Y.X., et al., *Improved gray wolf particle filtering and high-fidelity second-order autoregressive equivalent modeling for intelligent state of charge prediction of lithium-ion batteries.* International Journal of Energy Research, 2021. **45**(13): p. 19203-19214.

[15]. Wu, X. and X. Zhang, *Parameters identification of second order RC equivalent circuit model for lithium batteries.* Journal of Nanjing University. Natural Sciences, 2020. **56**(5): p. 754-761.

[16]. Ji, Y.-j., S.-l. Qiu, and G. Li, *Simulation of second-order RC equivalent circuit model of lithium battery based on variable resistance and capacitance.* Journal of Central South University, 2020. **27**(9): p. 2606-2613.

[17]. Li, L., et al., *A Novel Online Parameter Identification Algorithm for Fractional-Order Equivalent Circuit Model of Lithium-Ion Batteries.* International Journal of Electrochemical Science, 2020. **15**(7): p. 6863-6879.

[18]. Hu, M., et al., *Lithium-ion battery modeling and parameter identification based on fractional theory.* Energy, 2018. **165**: p. 153-163.

[19]. Yuan, C., et al., *Remaining Useful Life Prediction and State of Health Diagnosis of Lithium-Ion Battery Based on Second-Order Central Difference Particle Filter %J IEEE*

Access. 2020. **8**.

[20]. Fan, T.E., et al., *Simultaneously estimating two battery states by combining a long short-term memory network with an adaptive unscented Kalman filter.* Journal of Energy Storage, 2022. **50**.

[21]. He, H., et al., *Comparison study on the battery models used for the energy management of batteries in electric vehicles.* Energy Conversion and Management, 2012. **64**: p. 113-121.

[22]. Bin, W., et al., *Adaptive state of energy evaluation for supercapacitor in emergency power system of more-electric aircraft.* Energy, 2023. **263**(PA).

[23]. Wang, Y., C. Zhang, and Z. Chen, *Model-based State-of-energy Estimation of Lithium-ion Batteries in Electric Vehicles.* Energy Procedia, 2016. **88**.

[24]. Peng, H., et al., *A SOE estimation method for lithium batteries considering available energy and recovered energy.* Proceedings of the Institution of Mechanical Engineers, Part D: Journal of Automobile Engineering, 2023. **237**(1).

[25]. Li, X., et al., *State of energy estimation for a series-connected lithium-ion battery pack based on an adaptive weighted strategy.* Energy, 2020.

[26]. Khaled, L. and M.C.A. J., *A review of supercapacitors modeling, SoH, and SoE estimation methods: Issues and challenges.* International Journal of Energy Research, 2021. **45**(13).

[27]. Liu, Y., et al., *Simulation and parameter identification based on electrochemical-thermal coupling model of power lithium ion-battery.* Journal of Alloys and Compounds, 2020. **844**.

[28]. Ma, L., C. Hu, and F. Cheng, *State of Charge and State of Energy Estimation for Lithium-Ion Batteries Based on a Long Short-Term Memory Neural Network.* Journal of Energy Storage, 2021. **37**.

[29]. Zhang, X., et al., *A novel method for lithium-ion battery state of energy and state of power estimation based on multi-time-scale filter.* Applied Energy, 2018. **216**.

[30]. Hanwei, Z., et al., *State-of-electrode (SOE) analytics of lithium-ion cells under overdischarge extremes.* Energy Storage Materials, 2023. **54**.

[31]. Xinan, Z., et al., *Innovative method for state of energy estimation based on*

improved Cubature Kalman filter. Journal of Physics: Conference Series, 2021. **1754**(1).

[32]. Xin, L., et al., *A novel method for state of energy estimation of lithium-ion batteries using particle filter and extended Kalman filter.* Journal of Energy Storage, 2021. **43**.

[33]. Xiao, Y., et al., *A novel fuzzy adaptive cubature Kalman filtering method for the state of charge and state of energy co-estimation of lithium-ion batteries.* Electrochimica Acta, 2022. **415**.

[34]. Wei, X., et al., *A Multi-Timescale Estimator for Lithium-Ion Battery State of Charge and State of Energy Estimation Using Dual H Infinity Filter.* IEEE Access, 2019. **7**.

[35]. L., M., H. C., and C. F., *State of Charge and State of Energy Estimation for Lithium-Ion Batteries Based on a Long Short-Term Memory Neural Network.* Journal of Energy Storage, 2021. **37**.

[36]. Lai, X., et al., *A novel method for state of energy estimation of lithium-ion batteries using particle filter and extended Kalman filter.* Journal of Energy Storage, 2021. **43**.

[37]. Wei, X., et al., *Unscented Particle Filter Based State of Energy Estimation for LiFePO4 Batteries Using an Online Updated Model.* International Journal of Automotive Technology, 2022. **23**(2): p. 503-510.

[38]. Zhang, Z., et al., *Estimation of state-of-energy for lithium batteries based on dual adaptive particle filters considering variable current and noise effects.* International Journal of Energy Research, 2021. **45**(11): p. 15921-15935.

[39]. Dong, G.Z., et al., *An online model-based method for state of energy estimation of lithium-ion batteries using dual filters.* Journal of Power Sources, 2016. **301**: p. 277-286.

[40]. Xie, Y., et al., *A new method of unscented particle filter for high-fidelity lithium-ion battery SOC estimation.* Energy Storage Science and Technology, 2021. **10**(2): p. 722-731.

[41]. Xueyi, H., et al., *An improved forgetting factor recursive least square and unscented particle filtering algorithm for accurate lithium-ion battery state of charge estimation.* Journal of Energy Storage, 2023. **59**.

[42]. Jia, J., et al., *Multi-Scale Prediction of RUL and SOH for Lithium-Ion Batteries*

Based on WNN-UPF Combined Model. Chinese Journal of Electronics, 2021. **30**(1).

[43]. Yan, Z. and H. Jingtao, *The Precise Positioning Algorithm Optimization Base on PSO-PF for Agricultural Machinery Navigation System.* Journal of Physics: Conference Series, 2019. **1213**(4).

[44]. Mao, X., S. Song, and F. Ding, *Optimal BP neural network algorithm for state of charge estimation of lithium-ion battery using PSO with Levy flight.* Journal of Energy Storage, 2022. **49**.